RSC Advances

PAPER

View Article Online
View Journal | View Issue

Cite this: *RSC Adv.*, 2020, **10**, 14347

Preparation of a nanoscale homogeneous energetic lead azides@porous carbon hybrid with high ignition ability by *in situ* synthesis†

Zhenzhan Yan, Li Yang, * Ji-Min Han,* Naimeng Song and Jianchao Liu

Received 11th February 2020
Accepted 2nd March 2020

DOI: 10.1039/d0ra01317j

rsc.li/rsc-advances

The ever-increasing demand for miniaturized explosive systems urgently calls for better performance studies through the synthesis of novel nanoscale materials. In this work, lead azide@porous carbon hybrids (LA@PC) are synthesized by *in situ* carbonization and azidation of a lead-containing cross-linked gel, in which the nanoscale LA is uniformly distributed on the porous carbon skeleton. The detailed characterization has shown that such outstanding performance stems from the LA nanoscale effect and the excellent conductivity and thermal conductivity of carbon cages. Because of the favorable unique structure, the prepared composite material exhibits excellent ignition performance, and its flame sensitivity can reach 42 cm, which solves the problem of poor ignition capacity of LA on all occasions. In addition, the composite has very low electrostatic sensitivity, further improving the safety of practical application. This work makes it possible for LA to be detonated without using lead styphnate, paving a new way for improving the flame sensitivity of primary explosives.

Introduction

As the energy source for various ignition and detonation equipment, primary explosives are indispensable in explosive systems, because they are sensitive to the outside world and can be detonated by a smaller simple initial energy (flame, impact, acupuncture, friction, *etc.*).[1–3] At present, although a lot of new primary explosives have been developed, many factors still need to be considered and optimized for their practical applications, such as synthetic difficulties, high costs, and safety issues.[4–7] The combination of lead azide (LA) and lead styphnate (LS) represents one of the most widely used primary explosives.[8,9] Among them, LA has a strong detonating ability, but is vulnerable due to its poor ignition ability. Therefore, LA needs to be equipped with LS which exhibits a good ignition capacity and serves as the most commonly used ignition agent. However, in such an explosive system, the electrostatic sensitivity of the LS is extremely high, resulting in many terrible explosion accidents ascribable to static electricity.[10–15] The safety of the primary explosives (LS/LA, *etc.*) becomes a research bottleneck that needs to be addressed.

Various methods are employed to modify the primary explosives, including mixing antistatic agents and a crystal form controlling agents, physically doping conductive materials (carbon materials), and *in situ* chemical synthesis of hybrid explosives with carbon materials. For example, many new lead azide derivatives have been developed by adding dextrin, carboxymethyl cellulose, *etc.* during the preparation of lead azide.[16–20] Zhimin Li *et al.* doped graphene nanoplates during the preparation of lead azide and lead styphnate to reduce their electrostatic sensitivity.[21,22] However, the preparation of the primary explosives by the physical mixing method may have some problems such as poor uniformity of the sample, high cost, and high risk in the preparation process. Qianyou Wang *et al.* prepared a composite of copper azide (CA) uniformly distributed on the carbon skeleton by carbonization and *in situ* azidation of copper-containing metal organic frameworks (MOFs) as the precursor, which reduced the electrostatic sensitivity of copper azide.[23] The *in situ* synthesis method can avoid problems such as uneven physical mixing of the primary explosives particles on the carbon skeleton. However, the application of MOFs is strickly limited, because of the more complicated requirements for synthesis conditions, including temperature, mixed solvents, *etc.* Therefore, there is an urgent need to develop a cheap and simple synthesis strategy to modify primary explosives. Fortunately, in our previously reported work, copper azide@porous carbon hybrids (CA@PC) complex with nano-scale CA uniformly distributed on the carbon skeleton was feasibly prepared from a cheap and readily available gel.[24] This method has provided a new idea to improve the flame sensitivity of LA and may fundamentally solve the safety problem of the LA/LS system.

Herein, we applied the *in situ* synthesis method for the first time to prepare a carbon-based lead azide composite by

State Key Laboratory of Explosion Science and Technology, Beijing Institute of Technology, 5 South Zhongguancun Street, Beijing, 100081, P. R. China. E-mail: yanglibit@bit.edu.cn

† Electronic supplementary information (ESI) available. See DOI: 10.1039/d0ra01317j

carbonization and *in situ* azidation reaction using a cheap and readily available lead-containing hydrogel template. This *in situ* synthesis method not only excluded the usage of the sensitive LS, but also ensured the nano-scale lead azide uniformly attached to the porous carbon skeleton. In such a composite system, the size of LA is reduced to the nanometer scale, leading to the smaller decomposition potential energy and the advanced thermal decomposition temperature. Besides high specific surface areas, excellent electrical conductivity, and thermal conductivity,[23,25,26] the porous carbon skeleton can also provide binding sites for LA, and can be obtained from inexpensive raw materials by the simple carbonization step.[27–32] Through this strategy, the flame sensitivity of the LA@PC material can be increased to 42 cm, while the ignition ability is comparable to the commonly used ignition powder LS. In addition, the LA@PC composite has a static sensitivity as low as 1.25 J and has a higher safety rating than previously reported LA modified materials. The synthesis of LA@PC solves the problem of LA ignition difficulties, making it possible to replace LS as ignition powder.

Experimental

Material and methods

Materials. Sodium polyacrylate (PAA) is purchased from Aladdin. Lead acetate ($Pb(OOCCH_3)_2 \cdot 3H_2O$), acetic acid and Stearic acid were of analytical grade and purchased from Beijing Chemical Works. Sodium azide was analytical grade and purchased from Xiya Reagent. Other chemicals were of analytical grade and used without further purification. All solutions were prepared with distilled water.

Characterizations. All FT-IR spectra were recorded using FT-IR spectrometer (Nicolet 170, SXFT/IR spectrometer, USA) from KBr discs in the range of 4000–400 cm^{-1}. *TG-DTG curves*: Thermogravimetric analysis (TG) of PAA-Pb gel powder was determined by STA6000 (PerkinElmer, USA) under a helium flow of 50 ml min^{-1}. The sample (12 mg) was heated from 40 °C to 600 °C at a heating rate of 10 °C min^{-1}. Differential scanning calorimetry (DSC) of LA@PC were determined by CDR-4P (INESA Instrument, China) with 10 °C min^{-1} while heated up to 500 °C in air atmosphere. The decomposition temperatures were given as peak maximum temperature. Scanning electron microscopy (SEM) was performed using S-4800 (HITACHI, Japan) at 15 kV with a point resolution of 1.0 nm. The samples were characterized by transmission electron microscopy (TEM) using Tecnai G2 F30 (FEI, USA) at 300 kV with a point resolution of 0.20 nm. Both SEM and TEM were equipped with an EDX/EDS system. X-ray photoelectron spectroscopy (XPS) measurements were performed with a Thermo Scientific Escalab 250Xi using the monochromatic Al Kα line (1486.7 eV). Powder X-ray diffraction patterns were carried out with a Bruker D8 Advance diffractometer using Cu Kα radiation ($\lambda = 1.5406$ Å) at 40 kV and 40 mA. *Element analysis and ICP*: C, N and H contents were measured by EuroEA Elemental Analyser. Cu content was measured by PE optima 7000 with the standard curve method. *Electrostatic sensitivity test*: The test parameters: the charge capacitance is 500 pF, the electrode gap length is 0.12 mm. Samples were tested using the up and down method for each condition, and the electrostatic sensitivity (E_{50}) for 50% probability of ignition was calculated. Flame sensitivity test: 20 mg of the complex was compacted to a copper cap under the press of 39.2 MPa and was ignited by black powder pellet. Samples were tested using the up and down method for each condition, and the flame sensitivity (H_{50}) for 50% probability of ignition was calculated.

Preparation of samples synthesis of PAA-Pb hydrogel. 6 ml of PAA was dissolved in 70 ml of distilled water with stirring to ensure uniform stirring. 0.5 acetic acid was then added with stirring to keep the system acidic. 4.2 g of lead acetate was dissolved in 60 ml of distilled water, and the solution was added dropwise to the PAA system to effect gelation. After grinding and stirring with a ball mill, the PPA-Pb hydrogel particles were homogenized and centrifuged to collect a solid. The collected solid hydrogel was added to distilled water for grinding or stirring to ensure that the system became homogenized again. The homogel was then centrifuged or allowed to stand, and the solid hydrogel was collected. The collected hydrogel is repeated for the above steps to remove impurity ions such as Na+ and CH_3COO^-. The repeatedly washed hydrogel was freeze-dried and then a white powder was collected.

Preparation of *in situ* PbO nanoparticles doping in porous carbon frameworks (PbO@PC). The freeze-dried PAA-Pb gel powder was carbonized at 800 °C for 30 min under a nitrogen atmosphere. The temperature was ramped at 5 °C min^{-1} and the product was naturally cooled to room temperature. The carbonized black loose powder was collected for azide.

Preparation of *in situ* lead azides@porous carbon hybrid (LA@PC). A two-necked flask was connected to an argon inlet valve and a glass tube (containing a cotton-based sample tube, sample tube opening). A mixture of sodium azide and excess stearic acid was added to the two-necked flask, and the mixture was reacted at 120 °C to form a hydrazoic acid gas. LA@PC is prepared by reacting azide gas with a sample (carbonized product) in a glass tube. Before the reaction, argon gas should be introduced to remove the air from the system. The glass tube should be reconnected with NaOH solution as a scrubber for unreacted HN_3 gas. After the completion of the reaction, argon gas was again introduced to discharge the unreacted HN_3 gas remaining in the system. **Caution**! Hydrazoic acid is highly toxic, and metal azides are always energetic and especially sensitive. The entire system must be set up behind an explosion proof shield in a well-ventilated hood. The obtained black fluffy powder should be taken lightly (Fig. S6†).

Results and discussion

The schematic synthesis process of LA@PC is illustrated in Fig. 1. First, we selected cheap sodium polyacrylate (PAA) as the precursor material, lead acetate as the crosslinking agent, and acetic acid to adjust pH. The sodium polyacrylate lead ion crosslinked gel was then prepared (Fig. 1a and b), in which the metal ions lead can be uniformly scattered in the flexible organic molecular skeleton (Fig. S1c†).[33–38] The detailed process and characterization are shown in ESI (Fig. S1 and S2†). Purified

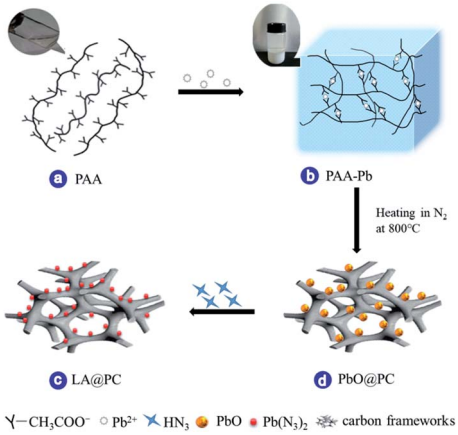

Fig. 1 Schematics of the synthesis process (a) the molecular structure of polyacrylic acid (PAA), inset is the digital image of PAA solution; (b) ionic-linked hydrogel prepared from PAA and Pb^{2+} (PAA-Pb), inset is the digital image of the formed hydrogel; (c) PbO nano-particles well-distributed in porous carbon frameworks (named as PbO@PC); (d) LA nano-crystals adhering to the porous carbon frameworks (named as LA@PC).

by repeated washing, the prepared crosslinked gel of polymers and lead ions exhibited the anti-swelling and self-healing properties. Through the strong hydrogen bonding with the hydrophilic $-COO^-$ groups, a large number of water molecules were locked in the three-dimensional polymer chains network to generate the desired hydrogel.[39,40] The porous dry gel framework was obtained by removing water after vacuum freeze-drying. After the ice crystals are sublimated, cavities were left at the position originally occupied by the water molecules in voids between polymer chains, and the metal ions are evenly distributed between organic molecular chains. The freeze-dried gel with rich pores provides a prerequisite for the smooth progress of the azide reaction, and it can also be stored under normal conditions for a long time without deterioration. Second, after the process of freeze-drying, powder of PAA-Pb gel was pyrolyzed at 800 °C for 30 min in nitrogen atmosphere. The resulting decomposition products were nanometer scale (about 30 nm) lead oxide uniformly distributed on the carbon skeleton. Detail characterization and morphology of PbO@PC are shown in support information (Fig. S3†). The performance of obtained composite material was compared with the raw material lead pyrolysis product under the air atmosphere (Fig. S4†). The decomposition product in the air atmosphere has a particle diameter of about 1 μm, probably because of the lead oxide agglomeration after the oxidization of the carbon skeleton, which is not suitable as a raw material for preparing nano-scale lead azide. Thirdly, through the course of the azidation reaction, lead azides@porous carbon hybrid (LA@PC) was prepared, in which nano-scale LA is evenly distributed in the carbon skeleton.

It can be seen from the TEM image in Fig. 2a–c that the particle size of the precursor material PAA-Pb, PbO@PC, and LA@PC are 20 nm, 30 nm, and 110 nm, respectively. Since the copper-containing gel particles (PAA-Pb) and the carbonized intermediate particles (PbO@PC) are both 20–30 nm, which is sufficiently small, the size of LA@PC can reach nanoscale (about 110 nm). From the particle size distribution map (Fig. 2e), D_{50} of LA@PC is about 120 nm. Compared with the particle size of LA (about 1 μm),[14] which is prepared by the reaction of sodium azide and lead nitrate, the size of LA@PC particle is greatly reduced. Elemental mapping (Fig. 2d) indicates that LA@PC is mainly composed of C, O, N, and Pb, among which N and Pb are dispersed uniformly throughout the porous carbon framework. In the PXRD analysis (Fig. 2f), the peaks related to PbO disappeared, while the typical $Pb(N_3)_2$ patterns emerged in the LA@PC complex, indicating that PbO is completely converted into LA. Furthermore, the characteristic peaks of divalent lead ions and azide anions can be clearly seen in the XPS spectrum of LA@PC (Fig. 2g, h and S5†). The data proved that the final sample is LA@PC composite, while the impurities such as PbO are not observed. The elemental analysis (EA) and inductively coupled plasma (ICP) emission spectrometer analysis indicate LA and carbon contents are 83.5% and 16.5%, respectively. The differential scanning calorimeter (DSC) curve in Fig. 2i exhibits three peaks according to thermal decomposition of LA at 229 °C, 352 °C, and 431 °C, respectively. It is worth noting that the three exothermic peaks in the DSC of LA@PC have different degrees of advancement compared with the conventional LA,[14] which may be related to the particle size reduction and the good thermal conductivity of the carbon skeleton.

Since LA's ignition ability is poor, in practical applications, LA must be used together with LS as the ignition powder. The high static sensitivity of LS brings great security risks to LS/LA. In order to compare the ignition capability and safety performance between the nano-sized LA@PC thus prepared and the rational LS/LA system, the same methods and equipment reported in our recent work are used to test the flame sensitivity and electrostatic sensitivity.[24] The value of H_{50} (flame sensitivity) corresponds to the height from standard black powder pellets to sample for 50% probability of ignition, revealing the ignition ability of the primary explosives. From Fig. 3a, the pure LA flame sensitivity is only 8 cm. The H_{50} values of LS/LA at 1 : 2 and 1 : 3 are 27 cm and 21 cm, respectively. Although the flame sensitivity of LS/LA at 2 : 1 and 3 : 1 reaches 40 cm and 42 cm respectively, since LS is the main component, the detonation ability and safety performance are greatly reduced. Proudly, the H_{50} can reach 42 cm LA@PC (carbon content only 16.5%) with excellent ignition capability, comparable to LS. To further compare the safety performance of the LA@PC and LS/LA systems, the electrostatic sensitivity of LA@PC was tested by a quantitative electrostatic stimulus, shown as E_{50} (the energy for 50% probability of ignition, mJ). The schematic diagram of the electrostatic sensitivity test principle is shown in Fig. 3b. As shown in Fig. 3c, the values of the LS and LA mixtures at different ratios of 3 : 1, 2 : 1 and 1 : 1 were 0.23, 0.61 and 1.15 mJ, respectively, the high electrostatic sensitivity in the LS/LA system is due to the presence of LS. Surprisingly, compared to pure LA and LS/LA system, the electrostatic sensitivity of LA@PC reached 1.25 J, which means the new LA@PC variety exhibits higher safety performance. Similarly, it can be seen

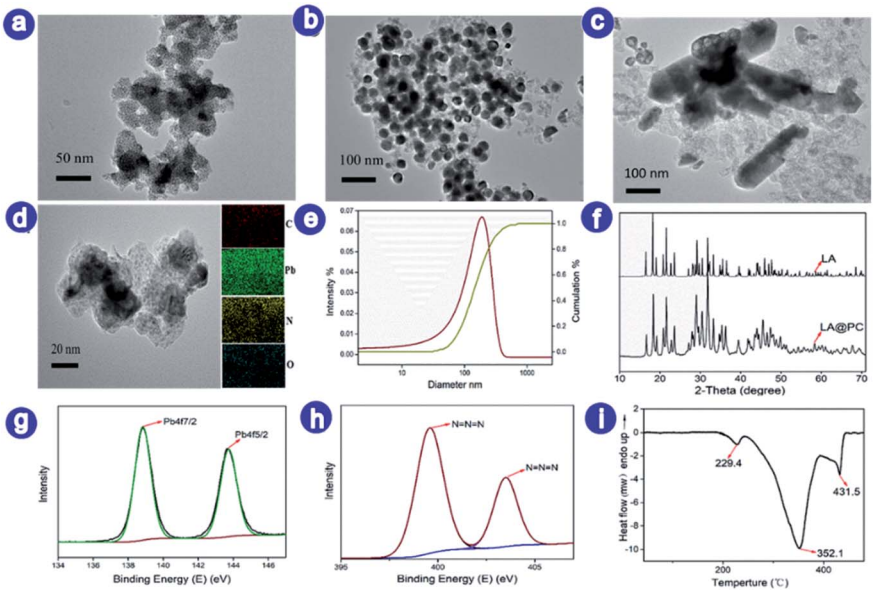

Fig. 2 (a) TEM image of PAA-Pb; (b) TEM image of PbO@PC; (c) and (d) TEM image and energy dispersive X-ray spectroscopy (EDS) mapping of LA@PC; (e) particle size distribution curves of LA@PC; (f) P-XRD pattern (JCPDS card no. 14-0629); (g) and (h) XPS spectra (Pb and N) curves of LA@PC; (i) DSC curve of LA@PC.

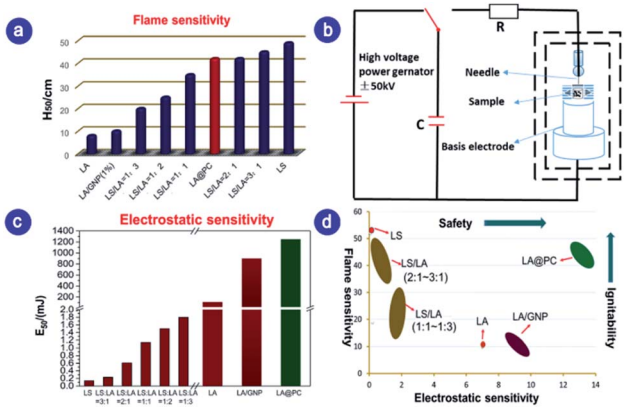

Fig. 3 (a) Flame sensitivities of LA@PC and the mixtures of LS/LA, respectively; (b) schematic diagram of electrostatic sensitivity test mechanism; (c) electrostatics sensitivities of LA@PC and mixtures of LA and LS, respectively; (d) the whole sensitivities comparison of LA@PC, LA, LS, LA/GNP, mixtures of LS/LA.

from Fig. 3d that LA@PC has the most excellent ignition capability and safety performance, compared with the ignition and safety performance of LA, LA/GNP, LS, LA and LS hybrid systems, which is of great significance in practical applications.

Comparing and analyzing the differences in scale, structure and sensitivity performance of primary explosives such as LA, LS/LA, and LA/GNP, we proposed the plausible mechanism of LA@PC flame sensitivity and electrostatic sensitivity reduction.

Fig. 4a is a schematic diagram of the mechanism of the increase in flame sensitivity. As we know, the thermal conductivity of lead azide is poor. If the flame contacts the bulky lead azide aggregates, the heat cannot be dispersed in time, resulting in poor ignition capability of the lead azide. However, for the prepared LA@PC sample, the LA is uniformly dispersed at the nanometer-scaled carbon frameworks. As the LA size becomes smaller, the number of atoms on the surface and the specific surface area increases. In addition to the high thermal conductivity of carbon material, the energy barrier to be overcome by each LA particle decomposition becomes smaller and

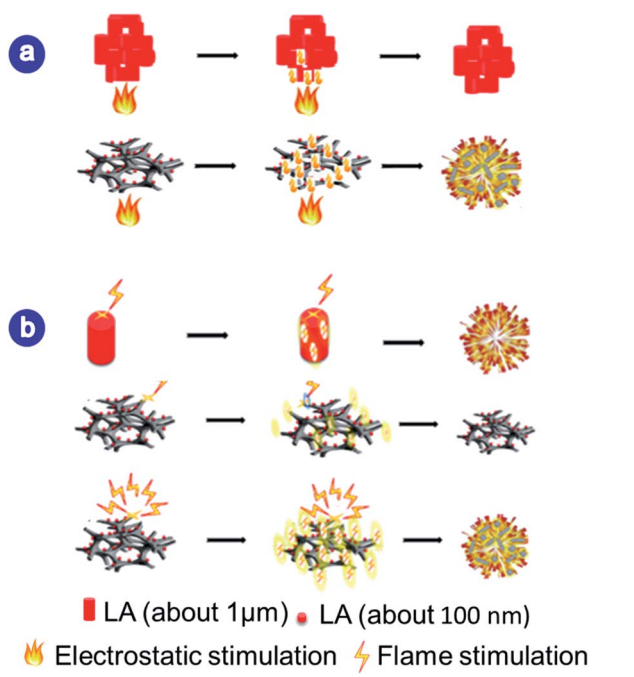

Fig. 4 (a) Schematic diagram of the mechanism of rising flame sensitivity; (b) schematics illustration of the mechanism of electrostatic sensitivity for LA.

the heat transfer efficiency is increased, which makes a small amount of heat sufficient for the LA to be rapidly decomposed in a short time, resulting in an increase in the flame sensitivity of LA@PC. Therefore, the thermal conductivity of the carbon skeleton and nanoscale LA is the key to the increase in flame sensitivity. Moreover, the schematic diagram of the mechanism of electrostatic sensitivity reduction of LA@PC is shown in Fig. 4b. Since the large particles of LA are gathered together, the static charge cannot be guided away in time, which leads to the electrostatic explosion to a large extent. However, when the nano-scale LA is uniformly dispersed on the carbon skeleton, the carbon skeleton is equivalent to the nano-scale Faraday cage, which can lead a part of the electric charge, reducing the possibility of explosion due to static electricity and improving the safety of the system. Therefore, it is believed that the porous carbon skeleton and uniform distribution of LA are the main reason for the low sensitivity of LA@PC.

Conclusions

In summary, we first prepared LA@PC by *in situ* azidation and carbonization of low-cost PAA-Pb hydrogel, in which nanoscale LA was uniformly distributed on the oxygen-rich porous carbon skeleton. The prepared LA@PC composite has lower electrostatic sensitivity and high ignition capability, and the flame sensitivity can reach 42 cm, which makes it possible for lead azide to be used without the ignition powder LS. The synthesis of LA@PC solves the problem that the pure lead azide flame has low flame sensitivity and poor ignition ability, and has high research value and application prospect.

Conflicts of interest

There are no conflicts to declare.

Acknowledgements

We gratefully acknowledge financial support from the National Natural Science Foundation of China (No. 11672040), the State Key Laboratory of Explosion Science and Technology (No. YB2016-17), and Beijing Institute of Technology Research Fund Program for Young Scholars.

References

1 J. W. Fronabarger, M. D. Williams, W. B. Sanborn, J. G. Bragg, D. A. Parrish and M. Bichay, *Propellants, Explos., Pyrotech.*, 2011, **36**, 541.
2 L. Zhai, X. Fan, B. Wang and F. Bi, *RSC Adv.*, 2015, **5**, 57833–57841.
3 N. Mehta, K. Oyler, G. Cheng, A. Shah and Z. Anorg, *Allg. J. Chem.*, 2014, **640**, 1309–1313.
4 D. Chen, H. W. Yang and Z. X. Yi, *Angew. Chem., Int. Ed.*, 2018, **57**, 2081–2084.
5 W. Li, K. C. Wang and Q. H. Zhang, *Cryst. Growth Des.*, 2018, **18**, 1896–1902.
6 D. Fischer, T. M. Klapötke and J. Stierstorfer, *Angew. Chem., Int. Ed.*, 2015, **54**, 10299–10302.
7 C. He and J. M. Shreeve, *Angew. Chem., Int. Ed.*, 2016, **55**, 772–775.
8 D. D. Ford, S. Lenahan, M. Jörgensen, P. Dubé, M. Delude and P. E. Concannon, *Org. Process Res. Dev.*, 2015, **19**, 673–680.
9 J. Giles, *Nature*, 2004, **427**, 580–581.
10 M. Krawiec, S. R. Anderson, P. Dubé, D. D. Ford, J. S. Salan, S. Lenahan, N. Mehta and C. R. Explos, *Pyrotech*, 2015, **40**, 457–459.
11 R. Matyas, J. Selesovsky and T. Musil, *J. Hazard. Mater.*, 2012, **213**, 236–241.
12 M. B. Talawar, A. P. Agrawal, M. Anniyappan, D. S. Wani, M. K. Bansode and G. M. Gore, *J. Hazard. Mater.*, 2006, **137**, 1074–1078.
13 E. Beloni and E. L. Dreizin, *Combust. Flame*, 2009, **156**, 1386–1395.
14 S. P. M. Bane, J. E. Shepherd, E. Kwon and A. C. Day, *Int. J. Hydrogen Energy*, 2011, **36**, 2344–2350.
15 D. Skineer, D. Olson and A. Block-Bolten, *Propellants, Explos., Pyrotech.*, 1998, **23**, 34–42.
16 M. Zhou, Z. Li and Z. Zhou, *Propellants, Explos., Pyrotech.*, 2013, **38**, 569–576.
17 G. W. C. Taylor, W. Abbey and S. E. Napier, Preparation of Explosive Substances Containing Carboxymethyl Cellulose, *US Pat.*, 3,291,664, Minister of Aviation in Her Britannic Majesty's Government of the United Kingdom of Great Britain and Northern Ireland, London, England, 1966.
18 R. Janardhanan, V. Vuayabasker and B. S. R. Reddy, *J. Am. Leather Chem. Assoc.*, 2012, **107**, 231–242.
19 J. Liu, Y. Jiang, W. Tong, T. Zhang and L. Yang, *Propellants, Explos., Pyrotech.*, 2016, **41**, 267–272.
20 G. W. C. Taylor, W. Abbey and S. E. Napier, Lead Styphnate Containing Methyl Cellulose, *US Pat*., 3,291,663, Minister of Aviation in Her Britannic Majesty's Government of the nitedKingdom of Great Britain and Northern Ireland, London, England, 1966.
21 Z.-M. Li, M.-R. Zhou, T.-L. Zhang, J.-G. Zhang, L. Yang and Z.-N. Zhou, *J. Mater. Chem. A*, 2013, **1**, 12710–12714.
22 Z.-M. Li, M.-R. Zhou and T.-L. Zhang, *Mater. Lett.*, 2014, **123**, 79–82.
23 Q. Wang, X. Feng, S. Wang, *et al.*, *Adv. Mater.*, 2016, **28**, 5837–5843.
24 R. Xu, Z. Yan, L. Yang, *et al.*, *ACS Appl. Mater. Interfaces*, 2018, **10**, 22545–22551.
25 By J. Lee, J. Kim and T. Hyeon, *Adv. Mater.*, 2006, **18**, 2073–2094.
26 M. Yang and Q. Gao, *Microporous Mesoporous Mater.*, 2011, **143**, 230–235.
27 Y. Mao, H. Duan, B. Xu, *et al.*, *Energy Environ. Sci.*, 2012, **5**, 7950–7955.
28 V. Pelletier, S. Bhattacharyya, I. Knoke, *et al.*, *Adv. Funct. Mater.*, 2010, **20**, 3168–3174.
29 W. Xia, B. Qiu, D. Xia, *et al.*, *Sci. Rep.*, 2013, **3**, 1935.
30 W. Xia, J. Zhu, W. Guo, *et al.*, *J. Mater. Chem. A*, 2014, **2**, 11606–11613.

31 O. Paris, C. Zollfrank and G. A. Zickler, *Carbon*, 2005, **43**, 53–66.
32 E. Raymundo-Piñero, F. Leroux and F. Béguin, *Adv. Mater.*, 2006, **18**, 1877–1882.
33 X. Yuan, D. C. Marcano, C. S. Shin, X. Hua, C. IsenhartL, S. C. Pflugfelder and G. Acharya, *ACS Nano*, 2015, **9**, 1749–1758.
34 H. Meng, P. Xiao, J. Gu, X. Wen, J. Xu, C. Zhao, J. Zhang and T. Chen, *Chem. Commun.*, 2014, **50**, 12277–12280.
35 N. Li and R. Bai, *Sep. Purif. Technol.*, 2005, **42**, 237–247.
36 J. Y. Sun, X. Zhao, W. R. Illeperuma, O. Chaudhuri, K. H. Oh, D. J. Mooney, J. V. Joost and Z. Suo, *Nature*, 2012, **489**, 133–136.
37 Z. Wei, J. H. Yang and Z. Q. Liu, *Adv. Funct. Mater.*, 2015, **25**, 1352–1359.
38 M. Ishihara, K. Nakanishi, K. Ono, M. Sato, M. Kikuchi, Y. Saito and A. Kurita, *Biomaterials*, 2002, **23**, 833–840.
39 Y. Liu, W. Wang and A. Wang, *Desalination*, 2010, **259**, 258–264.
40 N. A. Peppas, J. Z. Hilt and A. Khademhosseini, *Adv. Mater.*, 2006, **18**, 1345–1360.

